Int. J. Adv. Sci. Eng. *Vol.5 No.2 948-956 (2018)* 948 *E-ISSN: 2349 5359; P-ISSN: 2454-9967*

RESEARCH ARTICLE

Photovoltaic and Impedance Spectroscopy Analysis of ZrO_2/TiO_2 Composites for Dye Sensitized Solar Cells

S. Ranjitha[1]*, R. LavanyaDhevi[1], V. Hariharan[2]., P. M. Anbarasan[3]
R. Sathiya Priya[2], M. Sridharan[4]
[1]Department of Physics, Velalar College of Engineering and Technology, Erode, Tamilnadu, India.
[2]Center for Research and Development, Mahendra Engineering Colleges, Mallasamiduam, Namakkal – 637 503, Tamil Nadu, India
[3]Department of Physics, Periyar University, Salem, Tamil Nadu, India
[4]Department of Chemistry, SRM Institute of Science & Technology, Chennai, India

ABSTRACT: The nanostructured ZrO_2/TiO_2 samples were synthesized by hydrothermal method, sensitized with anthraquinone dyes and the photovoltaic property was studied. The photovoltaic cells were assembled and the short-circuit current of the devices was measured under continuous illumination at 100 mW/cm^2 corresponding to the twice of the standard solar light intensity. The observed results of photocurrent and transmittance measurements as a function of wavelength show good performance in the presence of anthraquinone dyes. The synthesized materials were characterized using X-ray diffraction, field-emission scanning electron microscopy, UV-visible spectrophotometry and electrochemical impedance spectroscopy. The results reveal that the absorption of anthraquinone dyes in ZrO_2/TiO_2 combinations were found to be efficient to increase the short-circuit photocurrent and open-circuit voltage of the cell. An optimal power conversion efficiency of 3% was obtained in a dye-sensitized solar cell (DSSC) containing the ZrO_2/TiO_2 film. The study concluded that the selected material combinations were promising for the enhancement of the conversion efficiency for the fabrication of high efficient, low cost and high stable DSSCs.

KEYWORDS: Anthraquinone, DSSC, ZrO_2, XRD, dyes, SEM, Solar Cells

https://doi.org/10.29294/IJASE.5.2.2018.948-956

© 2018 Mahendrapublications.com, All rights reserved

1. INTRODUCTION

At present, dye-sensitized solar cells (DSSCs) have attracted considerable attention due to its low cost compared with Si solar cell. The DSSC consisted of dye adsorbed TiO_2 thin film, a redox electrolyte and a counter electrode has focused on increasing the solar cell conversion efficiency by using the metal oxide semiconductor anode materials. Treatment of the photo anode with highly conducting materials into the photo electrode to increase electron transfer ability are particularly important for the improvement of photocurrent generation, fill factor and power conversion efficiency of DSSC's. The semiconductors such as TiO_2, ZnO, SnO_2, WO_3, etc., with suitable regenerative dyes ultimately convert solar irradiation into electricity. Moreover, TiO_2 is a wide band gap semiconductor and it has been used for a long time as photo electrode in DSSC. The advantage of TiO_2 is to absorb in UV region, slow electron transport ability and hence successfully used for the fabrication of solar cells. In order to increase more efficiency, there is an urgently need for high electron transport and well-suited photo anode [1-2]. Excluding TiO_2, it has previously been examined that the other metal oxide semiconductors such as SnO_2, Nb_2O_5 , ZnO and ZrO_2 are used as photo-anodes, but they have never been reported to be as Gratzel's photoanode. The aim of the current study was to introduce a wide band gap semiconductor combined with TiO_2 as a photoanode other than the semiconductors mentioned in the above discussion. Mixing of the oxides can produce new crystallographic phases with quite different properties than the original oxides. The use of mixed oxides in many technological fields is an attractive strategy to produce materials with superior properties than the single components. In particular, mixed oxides have been widely used in catalysis, because the surface characteristics of the individual oxides can be changed due to the formation of new sites in the interface between the components, or by the incorporation of one oxide into the lattice of the other The main reason was that the size difference between titanium and zirconium caused the increase of lattice parameters and cell volume leading to structure defects [3]. It has been reported that incorporation of ZrO_2 into TiO_2 leads to decrease in particle size of TiO_2 and increase in surface area due to the dissimilar nuclei and co-ordination geometry .mixture of ZrO_2 and TiO_2 was used as an electrode for dye-sensitized solar cell. Among all wide band gap semiconductors ZrO_2 are superior in its optical and electronic properties and it was made considerable attention of researchers which is used a main component in oxygen sensors, fuel cell electrolytes, catalysts and catalytic supports, metal

---

**Corresponding Author: Ranjilotus31@gmail.com*

Received: 12.10.2018 **Accepted:** 11.11.2018 **Published on**: 27.11.2018

oxide semiconductor devices, superior thermal and chemical stability to facilitate increase more efficiency, there is an urgently need for high electron transport and well-suited ZrO_2 and TiO_2 thin films, with their high refractive indices, low absorption in the visible and near-infrared spectral regions, good mechanical properties, as well as their high thermal and chemical stabilities, have been widely investigated for various optical applications in filters, lenses, waveguides, optical adhesives, anti-reflective coatings, and highly reflective coatings[4-7]. Neppolian et al [8] has reported that the small addition of ZrO_2 in TiO_2 prepared by aqueous sol-gel route effectively inhibits the phase transformation from anatase to rutile phase and increases the surface area which can be promoted the photovoltaic activity. Mixed ZrO_2/TiO_2 has been widely investigated in the photo catalysis field. The addition of small amounts of ZrO_2 in TiO_2 can prevent the anatase-to-rutile phase transformation. Therefore, the addition of ZrO_2 enhances the thermal stability of the phase transformation of pure TiO_2. Furthermore ZrO_2 has been used not only as a support for TiO_2 but also with TiO_2 as a binary oxide catalyst since ZrO_2 itself a photo catalyst and photosensitizer [9-10].A variety of techniques has been developed to prepare $ZrO_2$and TiO_2-based thin films, and composite ZrO_2–TiO_2 materials, among which the soft sol–gel route offers a number of advantages such as the excellent control on the film purity and homogeneity, low cost, abilities to deal with substrates of large area and/or complex shape, and the convenient fabrication of multi-component oxide films [11–12]. By far, a large number of researches have been devoted to the sol–gel preparation of ZrO_2, TiO_2, and ZrO_2–TiO_2 composite materials. However, among the available research papers concerning both the bulk and thin films of .The aim of the present is to bring out the preparation and characterization of ZrO_2 and TiO_2 added ZrO_2 thin film on FTO substrates, for the effective utilization of DSSC. Electrochemical Impedance spectroscopy (EIS) is one of the powerful techniques to investigate the kinetic processes. This method has used to identify the effects on DSSC performance of depositing ZrO_2 coatings on FTO of varying thickness on the TiO_2 nanoparticles with attention focused on the various interception processes. ZrO_2 with its lower electron affinity would have been a very promising entrant in DSSC in order to increase the V_{OC} of the device by increasing the negative value of conduction band. In case of only ZrO_2 as a photo anode, electron injection has not been reported even for commonly used ruthenium dyes [12–13].The efficiency of the device depends upon the sensitizer's anchoring group. The use of ruthenium complexes as sensitizers is expensive and unsuitable for environment, hence challenging the co-workers to search novel sensitizers. Qinghua Meng [14] proposed that anthraquinone structures naturally have an electron-withdrawing central ring and some electron-donating groups on the side-rings in structure of donor–acceptor–donor (D-A-D). He also reported that anthroquinone dyes have been used as sensitizers and it is widely used due to its high absorption coefficient, moderate oxidation/reduction ability, and low cost. J. Mech [15] reported that Anthraquinone derivatives onto the surface of nanocrystalline titanium dioxide reveal promising photoelectrochemical properties toward visible light and alternative for ruthenium complexes.

The best efficiency of DSSC, numerous groups have been analyzed and confirmed /that the nano-crystalline metal oxide doped thin films with a thin layer coating of a different metal oxide with a higher conduction and band-gap edge [16]. However, the process of preparing ZrO_2 / TiO_2 type semiconductor was complicated. Thus, we proposed the convenient alternative to enhance the efficiency of the DSSC. In this study, the photovoltaic characteristics of the DSSCs based electrode are reported in comparative mode by using TiO_2 which were synthesized from chemical route [17-20]. The electrode fabricated using TiO2–ZrO_2 gave better performances on both of short circuit current density and open circuit voltage [21]. The effects of Pure zirconia and doped with TiO_2 on current–voltage characteristics and fabricated by ZrO_2 / TiO_2 electrodes gave better performances on both of short circuit current density,open circuit voltage and low recombination rate.

EXPERIMENTAL PROCEDURE

2.1 Materials

The chemicals zirconium oxychlorideoctahydrate ($ZrOCl_2.8H_2O$), Titanium isopropoxide and Potassium hydroxide (KOH) were purchased from Sigma-Aldrich Chemicals and used as such for the preparation of pure ZrO_2. Fluorine doped Tin Oxide glass as a conductive transparency electrode was purchased from Pilkington, USA (8 X/cm). These substrates were utilized after cleaning by sonication in acetone (Fluke). The anthraquinone dyes such as Alizarin, Purpurin and Quinizarin were purchased from Sigma-Aldrich and Ruthenium-based dye (N719) was purchased from Solaronix, Switzerland. The dye was adsorbed from a 0.3 mM solution prepared by a mixed solvent of acetonitrile (Sigma-Aldrich) and tert-butylalcohol (Aldrich) with a volume ratio of 1:1.

2.2 Preparation of TiO_2 and ZrO_2 /TiO_2 Composites

About 1.1 ml of acetic acid was dispersed into 5 ml of Titanium isopropoxide and mixed for 30 minutes and added 50 ml of the deionized water under stirring to start the hydrolysis reaction. 1ml of nitric acid was added to resultant precursor solution and transferred into stainless steel teflon lined autoclave capacity of 100 ml and maintained in an oven at 200ºC for 24 hours. Final precipitate was centrifuged and washed several times with deionized water and acetone many times to make it free from chloride and organic impurities and then dried at 80ºC for 5 hrs. ZrO_2 doped TiO_2 nanoparticles were prepared as follows: 50 mg of the $ZrOCl_2.8H_2O$ was added into a 60 ml of water and 1.0 g of the prepared TiO_2 nanoparticle and continuously stirred for 1 hr. After the addition of NaOH solution, the sample was transferred into stainless steel teflon lined autoclave then followed the above mentioned procedure.

2.2 Fabrication of DSSC

The fabricated ZrO_2 and ZrO_2 / TiO_2 photoanodes and Pt coated counter electrode were assembled and sealed by a sealing surlyn sheet (SX 1170-60, Solaronix thickness of 60 lm) at 2 cm^2 x 2 cm^2. The electrolyte was injected to the cell through a small hole in the counter electrode. The holes were then covered by a small piece of microscopic glass with a surlyn sheet. The active area of the cell was adjusted to 0.25 cm^2 x0.25 cm^2. The preparation methods of ZrO_2 and ZrO_2 / TiO_2 are shown in Figure 1.

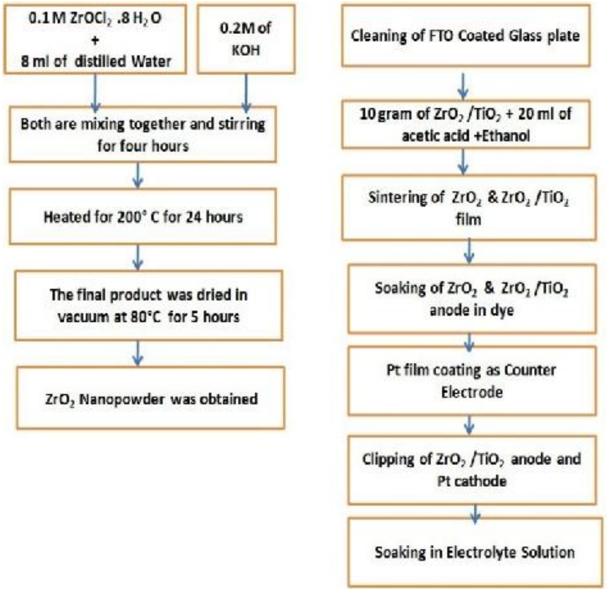
0.1 M ZrOCl₂ .8 H₂O + 8 ml of distilled Water
0.2M of KOH
Both are mixing together and stirring for four hours
Heated for 200° C for 24 hours
The final product was dried in vacuum at 80°C for 5 hours
ZrO₂ Nanopowder was obtained
Cleaning of FTO Coated Glass plate
10 gram of ZrO₂ /TiO₂ + 20 ml of acetic acid +Ethanol
Sintering of ZrO₂ & ZrO₂ /TiO₂ film
Soaking of ZrO₂ & ZrO₂ /TiO₂ anode in dye
Pt film coating as Counter Electrode
Clipping of ZrO₂ /TiO₂ anode and Pt cathode
Soaking in Electrolyte Solution

Figure 1 Flow chart of Preparation of ZrO_2 and DSSC Fabrication

2.3 Measurements

The crystalline phases and morphologies of the nanofiber-added TiO_2 photoelectrodes were analyzed using X-ray diffraction (XRD,Dmax/1200, Rigaku) and field emission scanning electron microscopy(FE-SEM, S-4700, Hitachi). The dye adsorption ability of TiO_2 and the ZrO_2 / TiO_2 composites (in powder form) were measured by an ultra violet visible (UVeVis) spectrometer (S-3100, Scinco). ACHI660 (Thermo-Oriel, USA) was used to evaluate the photo electro chemical properties of the DSSCs. A solar simulator (Thermo-Oriel, 1000WXe lamp, AM 1.5 filters) was used as the light source. The AC impedance of the DSSCs was also measured using the same setup in the frequency range of 0.01 Hze100 kHz at amplitude of 10 mV.

3. RESULTS AND DISCUSSION

3.1 Powder X-ray Diffraction (XRD) Analysis

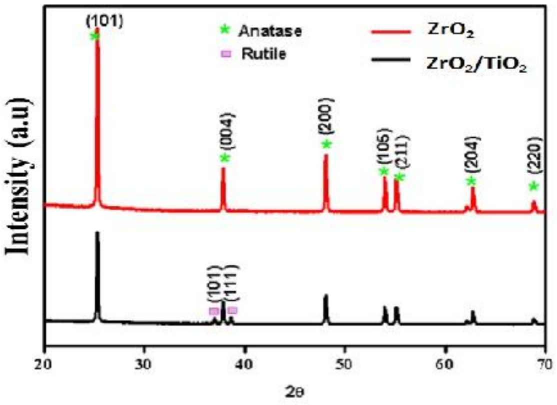

Figure 2(a and b): XRD pattern of ZrO_2 & ZrO_2 / TiO_2

The purity and crystallinity of the pure ZrO_2 and ZrO_2/ TiO_2 nanoparticles were examined by using powder XRD analysis. Figure 2(a & b) show the XRD pattern of pure TiO_2 and ZrO_2/TiO_2 nanoparticles, respectively. It can be seen from the Figure 2 (a) both of them indexed hexagonal phase of Titanium oxide (JCPDS card no. 79-1768) and ZrO_2/TiO_2 nanoparticles exhibits tetragonal phase with sharp diffraction peaks comparing than that of TiO_2, indicating the extremely small dimension of the ZrO_2/TiO_2 nanoparticles. The average crystalline sizes were calculated using Scherrer equation (1), the size was found to be 34 nm for ZrO_2 and 18 nm for ZrO_2 / TiO_2 exhibit respectively, in the structure of TiO_2 anatase (1 0 1), (2 11) ZrO_2/ TiO_2 rutile (1 0 1), (1 1 1). The TiO_2 exists in the anatase phase and the presence of Zr prevents the phase transformation from anatase to rutile. In fact under the specific preparation conditions, the films were comprised of anatase only and rutile phase was not detected. The Scherrer equation for determining the crystalline size as follows:

$$L = K\lambda/\beta\cos\theta \qquad \text{------ (1)}$$

Where K is a constant taken as 0.89, λ is the wavelength of the X-ray radiation (1.5418 Å), β is the full width at half maximum (FWHM) of the peak and θ is the diffracting angle.

The peak intensity at the most of the planes in ZrO_2/ TiO_2 decreased with increasing of zirconium content compared to that of pure TiO_2. Generally, domain sizes decreases with increasing of line broadening of the peaks, (101) index is related to size of the hexagonal crystalline phase [21-22]. As a result, there was a slight change in c parameter of the developed materials compared to the reference sample. The result can be considered as another proof regarding doping of Zr (+IV) in the TiO_2 matrix.

3.2 Field-Emission Scanning Electron Microscope (FESEM) Analysis

The surface morphologies of FTO coated pure ZrO_2 and ZrO_2/TiO_2 nanoparticles were studied by FESEM and the results are reported in Figure 3 (a & b). It can be seen that the grain sizes of FTO coated pure TiO_2 and ZrO_2/TiO_2 semiconducting nanoparticles annealed at 450ºC were found to be 10-20 nm, respectively. The ZrO_2 and ZrO_2 / TiO_2 particles exhibited uniform morphologies. However some aggregations were seen in ZrO_2 doped anatase TiO_2 nanoparticles as shown in the Figure 3(b). The rate of particle aggregation is a major factor that controls the morphology and crystalline structure of the final product [23]. Therefore, the substantial formation of the different morphologies in these samples can be described to the effect of Zr content. The result of energy dispersive X-ray spectroscopic (EDAX) analysis of pure ZrO_2 / TiO_2 nano powders were shown in Figure 3(c and d). Trace elements were estimated by determining the percentage abundance of elements such as Ti, O & Zr present in the sample.

Table 1 Crystal Parameters of ZrO_2 and ZrO_2 / TiO_2

Materials	**Crystal Structure**	**Lattice Parameters Å**	**Volume (Å)^3**	**Crystalline Size**
ZrO_2	Hexagonal	a=3.595Å c=5.184 Å	67.04	34 nm
ZrO_2-TiO_2	Tetragonal	a=3.785Å c=9.513 Å	(a)136.31	18 nm

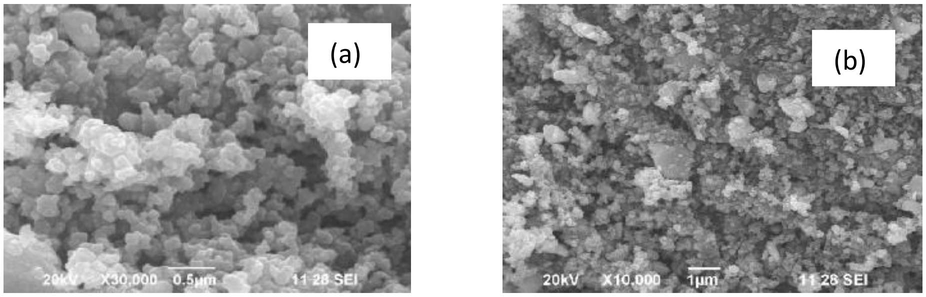

Figure: 3(a) FESEM Image of ZrO_2 film and (b) FESEM Image of ZrO_2 doped TiO_2

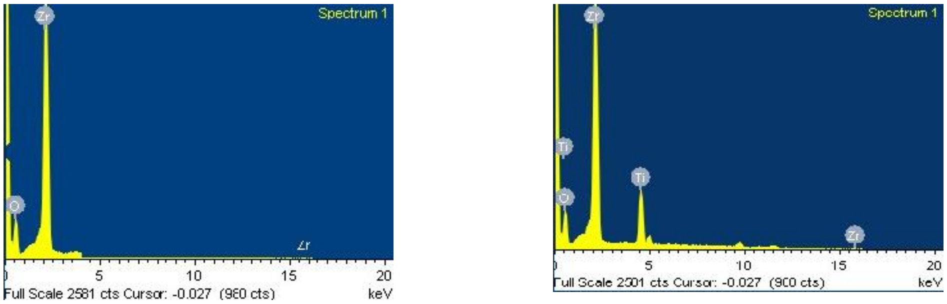

Figure: 3 (c and d) EDAX spectra of pure ZrO_2 and ZrO_2 doped TiO_2 film

3.3 UV-Visible Analysis

Figure 4(a) & (b) shows the absorption spectra of ZrO_2 and ZrO_2 / TiO_2. The absorption spectrum of antase ZrO_2 shows in the absorption wavelength from 327 to 400 nm towards visible region. When the electrons are excited, most of the electron from the conduction band of ZrO_2 can easily transfer to the conduction band of TiO_2 and hence, the band gap may be decreased for pure ZrO_2 is 2.95 eV and 1.95 eV respectively whereas the calculated band gap of ZrO_2 and ZrO_2 / TiO_2 is 2.8 eV and 1.91 eV and given in Table 2. The shift of the optical band gap edge towards longer wavelength has attributed to decreasing band gap. The absorption spectrum of anatase ZrO_2 shows a shift in the absorption edge towards longer wavelength region 437 nm, which might likely be caused by increasing in crystallite size, crystallinity and decreasing in band gap energy, whereas the ZrO_2/TiO_2 display a new absorption broads peak in the visible region from 437-648 nm.

The change in absorption maximum from 437 to 648 nm is attributed to the variation of energy level for the ZrO_2 /TiO_2 and the shift is due to the change in the energy of the lowest unoccupied molecular orbital (LUMO) of the metal oxide, causing the π-π^* and n-π^* transitions to occur at higher or lower energies. The shift in the absorption edge was found to increase with increasing concentration of ZrO_2/TiO_2 and reached a maximum at the optimum concentration. Further, ZrO_2 / TiO_2 imparts widening of spectral response covering complete visible region and extrapolation of the peak absorption edge results in a substantial decrease in band gap down to 1.91 eV (648 nm) [24-25]. This might be due to the fact that at higher concentration, ZrO_2/TiO_2 film absorbs more light.

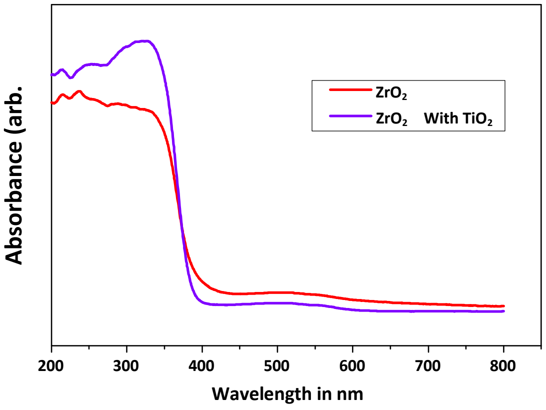

Figure 4 Absorption spectra of ZrO_2 & ZrO_2 doped TiO_2

3.4 Photoluminescence Analysis

In the room temperature Photoluminescence spectra two PL peaks were observed at 424 nm and 471nm under same excitation. All the samples have same broad band emission under excitation at 300 nm. However, the PL peak position and intensity are obviously different under different excitation wavelengths. The main peak is respectively located at about 424 and 471 nm under the excitation at 400 nm and 420 nm respectively.

Table 2: Band gap of ZrO_2 and ZrO_2/TiO_2

Materials	Optical band gap (eV)	Wavelength (nm)
ZrO_2	2.95	420
	1.95	634
ZrO_2/TiO_2	2.8	437
	1.91	648

The occurrence of emission peaks in the visible region was due to the presence of defects levels below the conduction band. The peak observed in the visible region has attributed to the electronic transition mediated by the defect levels such as oxygen vacancies in the band gap [27-28]. The first peak in PL spectra corresponds to band to band transition and the spectrum between 420–500 nm has been showing blue luminescence. As can be seen from the PL spectrum of hydrothermal derived nanoparticles, the high intensity peak was observed at 388.6 nm. PL spectrum of ZrO_2 / TiO_2 nanoparticles synthesized by solid state reaction method is shown in Figure 5(a&b). In TiO_2 exhibits a strong luminescence around 391.5 nm, which can be attributed to bound exciton emission. The PL intensity peak in case of solid state reaction synthesized nanoparticles was observed at 391.5 nm.

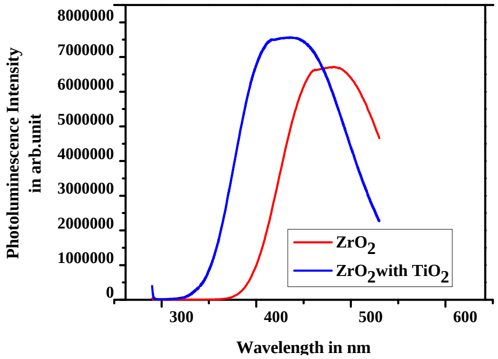

Figure 5: (a & b): PL spectra of ZrO_2 & ZrO_2 / TiO_2

3.5 Photovoltaic Characterization

These measurements were performed under '1 sun' illumination; however, few measurements were also carried out at other illumination intensities The open-circuit voltage (V_{oc}), short circuit current density (J_{sc}), fill factor (FF) and conversion efficiency of the samples ZrO_2 and ZrO_2/TiO_2 was given in the Table 3 and efficiency chart was comperd given in Figure 6 (a&b). The fill factor and efficiency were calculated from using different dyes measured under a stimulated illumination with a light intensity of 100 mW / cm^2. In principle, the maximum I_{sc} of a dye-sensitized solar cell was determined by how well the absorption window of the dye overlaps with the solar spectrum.

The experimental results given in table 3 shows that the existence of ZrO_2 / TiO_2 element provides more reactive vacant sites for the absorption of dye molecules that make the cell attract more photons and consequently produce a high density of electrons. In addition to that Zr-doped TiO_2 can boost the electron path from the photo-sensitizer to the FTO substrate in the DSSCs by reducing the recombination rate of electrons with the excited dye through the conduction band of TiO_2. According to the photovoltaic properties of the investigated material, ZrO_2 / TiO_2 enhance the absorption of visible light due to the formation of intermediate electronic levels between the conduction and valence bands of the metal oxide, and also decrease the charge recombination rate of electrons, which can be considered as the primary reason η to produce a high Jsc. Specifically, the enhanced photovoltaic efficiency was successfully achieved for the DSSC using ZrO_2 / TiO_2 as a photoanode at an optimum loading of Zr (1%) alizarin 0.86%, purpurin 1% quinazarin 1.2% and N719 dye 1.8% and The corresponding solar light-to-electricity conversion efficiency of new ZrO_2/TiO_2 structures for alizarin 0.96%, purpurin 1.1 % quinazarin 1.4% and N719 dye 2.5% were obtained respectively. The results of anthroquinone dyes compared with Ru complexes gave better efficiency which was reported earlier results.

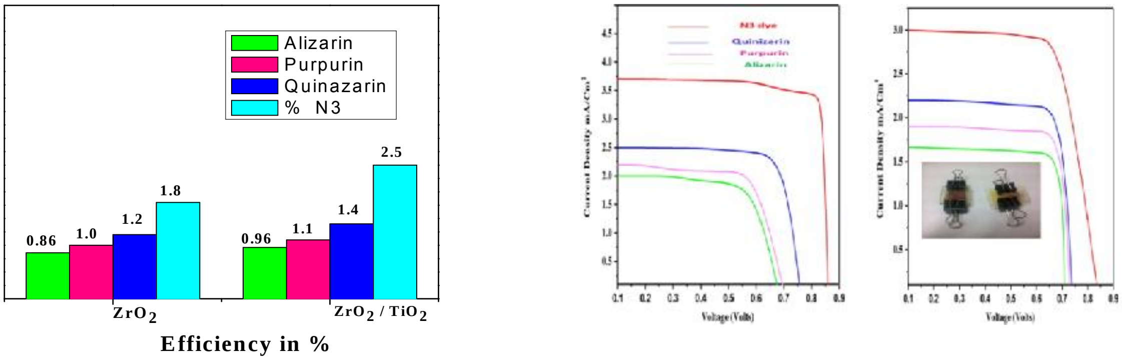

Figure 6 (a and b) Photovoltaic Parameters of DSSC for ZrO_2 and ZrO_2 / TiO_2

Table 3: The performance of dye-sensitized solar cells in terms of short circuit current density J_{sc}, open circuit voltage V_{oc}; fill factor FF and efficiency η (%)

Dyes	Compound	V_{oc} (V)	J_{sc} (mA/m^2)	Fill Factor	Efficiency (η in %)
Alizarin	ZrO_2	0.71	1.67	0.73	0.86
	ZrO_2/TiO_2	0.68	2.0	0.70	0.96
Purpurin	ZrO_2	0.72	1.9	0.74	1.0
	ZrO_2/TiO_2	0.70	2.2	0.75	1.1
Quinizan	ZrO_2	0.74	2.2	0.73	1.2
	ZrO_2/TiO_2	0.76	2.5	0.77	1.4
N3 dye	ZrO_2	0.84	3.0	0.70	1.8
	ZrO_2/TiO_2	0.86	3.7	0.80	2.5

3.3 Electrochemical Impedance Analysis of TiO_2 & ZrO_2/ TiO_2

The electrochemical impedance analysis was carried out for the samples ZrO_2 and ZrO_2 / TiO_2 using PARSTAT 2273 Advanced Electrochemical system (Princeton Applied Research) with frequency range from 1 Hz to 1 MHz. The Nyquist and bode phase plots have given in Figures 7(a,b) & 8(a,b). Figure 7(a) shows the Nyquist plot of the DSSCs configuration and impedance spectra obtained for ZrO_2 passivated ZrO_2/TiO_2 photoanode. The fitted data of the R_s and R_{ct}, τ_s, τ_n and η_c obtained from the Nyquist plots were reported in the Table 5. The Nyquist plot of second semicircle indicates that the electron transport in the Zr doped TiO_2 interface has reduced as compared with pure ZrO_2. Here, the Nyquist plot displays the impedance behavior of an interfacial electrochemical response among cell elements in an equivalent circuit. The impedance spectra consist of three distinct semicircles in a complex plane situated in high, intermediate, and low frequency regimes. The high frequency semicircle (I) to the charge transfer resistance at the electrolyte/platinum counter electrode [26-29]. The semicircles (II and III) at the intermediate and low frequency range correspond to charge transfer resistances at the photoanode/dye/electrolyte interface and the Nernst diffusion of the redox couple within the electrolyte respectively. Nyquist plots fitted to the equivalent circuit represented in Fig. 8. As illustrated, the overall equivalent circuit model composed of one R–C loops with electrochemical parameters R_1, C_1, and $R_2$is in series with the ohmic resistance, R_{ohm}. The electron charge transfer at electrolyte/platinum counter electrode and photoanode/dye/electrolyte interfaces are represented by R_1 and R_2, respectively. Thus, the EIS data were analyzed by fitting to an equivalent electrical circuit model [30-33].The resistances obtained were normalized to the geometric active surface area. The total resistance is sum of all the contribution of R_s and R_{ct} and the recombination time $\boldsymbol{\tau_s}$ was reduced from 2.7 sec for ZrO_2 and 1.15 sec for ZrO_2/ TiO_2 to minimize the total resistance in the cell. The charge collection efficiency $\boldsymbol{\eta_c}$ of thin ZrO_2 doped TiO_2 electrode was remarkably better than the pure ZrO_2 increases with from 44% to 72%.

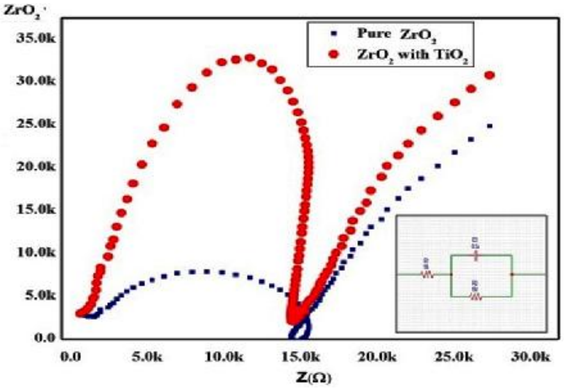

Figure 7 (a &b) Nyquist plots of DSSCs with ZrO_2/TiO_2

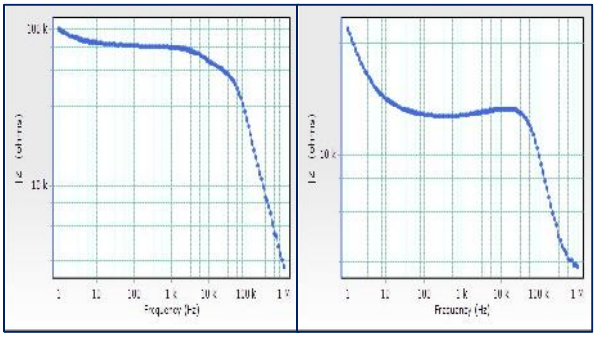

Figure 8 (a&b) Bode plots of DSSCs with ZrO_2 and ZrO_2 / TiO_2

Table 5: Electrochemical impedance analysis results of pure TiO_2 and ZrO_2 doped TiO_2

Sample	R_s (Ω)	R_{ct} (Ω)	τ_s (sec)	τ_n (sec)	η_c (%)
ZrO_2	9.79	7.85	2.78	2.23	44
ZrO_2/TiO_2	12.01	32.60	1.15	3.14	72

4. CONCLUSION

The nanoparticles of TiO_2 and ZrO_2 / TiO_2 were prepared by sol-gel method and characterized using powder XRD, UV, FT-IR, FE-SEM, EDAX, PL, Electrochemical Impedance Analysis and Photovoltaic performance. The average crystallite sizes of TiO_2 and ZrO_2 / TiO_2 was 20 nm and 14 nm, respectively. The prepared electrodes with TiO_2 and ZrO_2 / TiO_2 by sol–gel method were applied to these electrodes to the photo anode of a DSSC.

When the photoanode was immersed in anthroquinone dyes, the efficiency values are increased when compared with TiO_2 and ZrO_2/TiO_2. It was confirmed that the efficiency improvement is shown in the chart was attributed to the increase in the dye adsorption in ZrO_2 / TiO_2 plate than TiO_2 and enhancement in the V_{oc} was caused by the conduction band edge shift of ZrO_2 doped TiO_2 by decreasing of band gap from 2.95 eV to 2.8 eV. The conversion efficiency of Zr doped TiO_2 with anthraquinone dyes and the standard N3 dye was a promising material for enhancing the conversing energy by chemical preparation method. The electrochemical impedance analysis shows significant results in longer electron lifetime (τ_n), faster electron transport time (τ_s) and charge collection efficiency (η_c) for ZrO_2 / TiO_2 than TiO_2 based DSSCs with efficiencies 44% and 72%.

REFERENCES

1) O'Regan, B, Grätzel,M,1991. A low-cost, high-efficiency solar cell based on dye-sensitized colloidal TiO_2 films, Nature 353, 737–740.
2) Bach,U., Lupo,D., Comte,P., Moser,J.E., Weissörtel,F., Salbeck, J., Spreitzer, H., Grätzel, M,1998. Solid-state dye-sensitized mesoporous TiO_2 solar cells with high photon-to-electron conversion efficiencies, Nature, 395, 583-585.
3) Zhang,J., Vlachopoulos, N., Hao,Y., Holcombe, T.W., Boschloo,G., Jonhansson, E.M.J., Grätzel, M., Hagfeldt, A.,2016. Efficient Blue-Colored Solid-State Dye-Sensitized Solar Cells: Enhanced Charge Collection by Using an in Situ Photoelectrochemically Generated Conducting Polymer Hole Conductor, Chem.Phys.Chem 17, 1441-1445.
4) Tahir, MN, Gorgishvili, L, Li, J, Gorelik, T, Kolb, U, Nasdala, L & Tremel, W 2007, Solid State Science, 9, 1105-1109.
5) Durr M, S. Rosselli, A. Yasuda, G. Nelles, Band-gap engineering of metal oxides for dye-sensitized solar cells, J. Phys. Chem. B 110(2006) 21899–21902.
6) Adachi, M, Okada, I., Ngamsinlapasathian, S., Murata, Y. and Yoshikawa, S. Dye sensitized solar cell using semiconductor thin film composed of titania nanotubes, Electrochemistry, 70(2002) 449-452.
7) Jifa Qi, Xiangnan Dang, Paula Hammond, T., Angela Belcher, M 2011. Highly efficient plasmon-enhanced dye-sensitized solar cells through Metal Oxide Core Shell Nanostructure, ACS nano, 5(9) 7108-7116.
8) Neppolian B, Q. Wang, H. Yamashita and H Choi,2007.Synthesis and characterization of ZrO2–TiO2 binary oxide semiconductor nanoparticles: Application and interparticle electron transfer process, Appl. Catal. A, 333, 264–271.
9) Khan M.M, S.A. Ansari, D. Pradhan, M.O. Ansari, D.H. Han, J. Lee, M.H. Cho,2014. J. Mater. Chem.A 2, 637–644.
10) Tian G, K. Pan, H. Fu, L. Jing, W. Zhou, 2009. Enhanced photo catalytic activityof Sdoped TiO_2–ZrO_2 nanoparticles under visible light irradiation. Hazard. Mater, 166, 939–944.
11) Win, T. T., Maung, Y. M., Soe, K. K. K.2012. Fabrication of TiO_2-ZrO_2 Binary Oxide Electrode with Natural Dye (Rose) for Dye Sensitized Solar Cell Application. Advanced Materials Research Journal, 550, 2036-2039.
12) Qiao K, Hu N,2009. Direct electron transfer and electrocatalysis of myoglobin loaded in layer-by-layer films assembled with nonionic poly(ethylene glycol) and ZrO2 nanoparticles, Bioelectrochemistry, 75,71-76.
13) Chang S.M, R.-a.2006. Doong,Characterization of Zr-doped TiO_2 nanocrystals prepared by a nonhydrolytic sol–gel method at high temperatures, J. Phys. Chem. B 110, 20808–20814.
14) Qinghua Meng, Wenfan Yan, Meijuan Yu, Deyin Huang ,2003. A study of third-order nonlinear optical properties for anthraquinone derivatives, Dyes and Pigments 56 145–149.
15) J. Mech and K. Szaciłowski,2013.New Type of Photoactive Materials Based on TiO_2 Modified by Anthraquinone Derivatives, Archives of Metallurgy and Materials, 58: 269–273.
16) M. H. Liao, C. H. Hsu, and D. H. Chen,2006. Preparation and properties of amorphous titania-coated zinc oxide nanoparticles, Journal of Solid State Chemistry,179, 2020–2026,.
17) Geeta, M., Suguna, K., Anbarasan, P.M.,Aroulmoji, V, 2014. Preparation and characterization of tailored TiO2 nano particles for dye sensitized solar cells. Int.J.Adv.Sci.Eng, 1(1) 1-5.
18) Joo,J, T. Yu, Y.W. Kim, H.M. Park, F. Wu, J.Z. Zhang., T. Hyeon, 2003.Multigram scale synthesis and characterization of monodisperse tetragonal zirconia nanocrystal, J. Am. Chem. Soc., 125, 6553–6557.
19) Laxmi J. Tomar, B.S.Chakrabarty,2013. Synthesis,structural and optical properties of TiO_2-ZrO_2 nanocomposite by hydrothermal method' Adv. Mat.Lett. 4, 64-67.
20) C. McManamon, J. D., Holmes., M. A. Morris, 2011. Improved photocatalytic degradation rates of phenol achieved using novel porous ZrO_2-doped TiO_2 nanoparticulate powders, Journal of Hazardous Materials, 193,120–127,
21) Shao G.N, A. Hilonga, S.J. Jeon, J.E. Lee, G. Elineema, D.V. Quang, J.-K. Kim, H.T. Kim,2013. Influence of titania content on the mesostructure of titania–silica composites and their photocatalytic activity, Powder Technol. 233,123–130.
22) Zou, H & Lin, YS 2004, Structural and surface chemical properties of sol–gelderived TiO_2/ZrO_2 oxides, Appliled Catalysis. A Geneneral, 265, 35-42.
23) Htet Nwe, Yin Maung Maung, Than Than Win & Ko Ko Kyaw Soe 2012, 'Photovoltaic properties of mesoporous TiO_2–ZrO_2 binary oxide electrode with sawdust organic dye for dye-sensitized

solar cell application, Journal of Science (JOS) 197, 3(1), 2324-9854.

24) Laxmi J Tomar., Chakrabarty, BS 2013, Synthesis, structural and optical properties of TiO_2/ZrO_2 nanocomposite by hydrothermal method, Advanced Materials Letters, 4(1), 64-67.

25) Menzies, D, Cervini, R, Cheng, Y, Simon, P & Spiccia, L 2004. Nanostructured ZrO_2-coated TiO_2 electrodes for dye-sensitized solar cells, Journal of Sol–Gel Science Technology., 32, 363-366.

26) Pecharroman, C, M. Ocana and C.J. Serna, 1996. Optical constants of tetragonal and cubic zirconia in the infrared, J. Applied Phys.80, 3479–3483.

27) Zhang,D., Zeng,F,2010. Structural, photochemical and photocatalytic properties of zirconium oxide doped TiO_2nanocrystallites, Applied Surface Science 257, 867–871.

28) Anandan,K.,Rajendran,V,2013. Low-temperature Synthesis and Characterization of Tetragonal-ZrO_2 Nanoparticles via Simple Hydrothermal Process, Journal of Physical Sciences, 17, 179-184A

29) Kim,S, M. Kang, 2011. Synthesis of Zr-incorporated TiO_2 using a solvothermal method and its photovoltaic efficiency on dye-sensitized solar cells, Bull. Korean Chem. Soc. 32 317–3322

30) Kitiyanan, A., Ngamsinlapasathian, S., Pavasupree, S.,Yoshikawa, S.2005. The preparation and characterization of nanostructured TiO_2–ZrO_2 mixed oxide electrode for efficient dye-sensitized solar cells, J. Solid State Chem., 178, 1044- 1048.

31) David, B, Menzies, A, Qing Dai, B,Yi-Bing Cheng, A, George, P, Simon, A, Leone Spiccia, B.,Menziesetal, DB 2006, One-step microwave calcination of ZrO2-coated TiO_2 electrodes for use in dye-sensitized solar cells incorporation in dye-sensitized solarcells, C.R. Chimie, 9, 713-716.

32) Jiao Wang, En Mei Jin, Ju-Young Park, Wan Lin Wang, Xing Guan Zhao., Hal-Bon Gu 2012, 'Increases in solar conversion efficiencies of the ZrO_2 nanofiber-doped TiO_2 photoelectrode for dye-sensitized solar cells , Nanoscale Research Letters, 7, 98, 1-4.

33) Baek, H.R., Eo. I.S, 2017. Electrochemical properties of TiO_2-metal oxide composites for dye-sensitized solar cell, Current Applied Physics 17,854-857

All © 2018 are reserved by International Journal of Advanced Science and Engineering. This Journal is licensed under a Creative Commons Attribution-Non Commercial-ShareAlike 3.0 Unported License.